Temperature-dependent magnetic properties of ultrathin Fe films: Interplay between local environment and itinerant ferromagnetism

R. Garibay-Alonso,[1] J. Dorantes-Dávila,[2] and G. M. Pastor[3]
[1]*Departamento de Investigación en Física, Universidad de Sonora, Apdo. Postal 5-88, Código Postal 83190, Hermosillo, Sonora, Mexico*
[2]*Instituto de Física, Universidad Autónoma de San Luis Potosí, Alvaro Obregón 64, San Luis Potosí, Mexico*
[3]*Centre National de la Recherche Scientifique, Laboratoire de Nanophysique Magnétisme et Optoélectronique, Institut National des Sciences Appliquées, 135 Avenue de Rangueil, 31062 Toulouse, France*
(Received 22 March 2006; published 22 June 2006)

The magnetic properties of ultrathin Fe films are determined as a function of temperature in the framework of a functional-integral itinerant-electron theory. The environment-dependent electronic structure is derived from a realistic *d*-band model and a real-space recursive expansion of the local Green's functions. The statistical average of spin fluctuations is performed within the static approximation and a layer-resolved alloy analogy by treating disorder in the virtual crystal approximation and in the coherent potential approximation. Results are given for the temperature dependence of the local moments, layer magnetizations $M_l(T)$, and spin fluctuation energies of ultrathin bcc (001) films. These are compared with the corresponding bulk results in order to quantify the role of dimensionality. Strain and local environment effects are quantified by varying the interatomic bond length d. A strong nonmonotonous dependence of $M_l(T)$ as a function of d is revealed, which can be correlated with the environment dependence of the electronic structure and with the resulting changes in the ground-state magnetic moments and spin fluctuation energies. Finally, goals, limitations, and possible extensions are briefly discussed.

DOI: 10.1103/PhysRevB.73.224429 PACS number(s): 75.70.Ak, 75.10.Lp, 75.50.Bb

I. INTRODUCTION

The magnetic properties of low-dimensional systems, nanoparticles, and nanostructures are a subject of central interest from both fundamental and technological standpoints.[1,2] In the case of transition metals (TMs) having delocalized itinerant electrons it is well-known that the local environment of the atoms and the dimensionality of the system play a crucial role in defining the most important magnetic properties at temperature $T=0$, for example, the magnetic moments, magnetic order, or magnetic anisotropy. This strong sensitivity of magnetism on the atomic environment has been exploited to develop new materials by controlling the system size, shape, and lattice structure or by manipulating strain and proximity effects at the interfaces between different magnetic and nonmagnetic elements.[1,2]

A similarly strong environmental dependence of the magnetic behavior is expected at finite temperatures, as already demonstrated by previous experimental[3–12] and theoretical studies.[13–24] However, simple general trends on the stability of magnetism at finite T, for example, as a function of local coordination number z_l and nearest-neighbor (NN) distance d, are difficult to infer *a priori*. On the one side, one generally observes that the local magnetic moments M_l and d-level exchange splittings $\Delta\varepsilon_{Xl}^d=\varepsilon_{l\downarrow}^d-\varepsilon_{l\uparrow}^d$ at $T=0$ are enhanced as z_l is reduced or as the interatomic distances are increased.[25] On these grounds one would then expect that the stability of ferromagnetism, as given by the low-temperature decrease of $M(T)$ or by the Curie temperature T_C, should be stronger in low-dimensional systems than in the periodic solid. However, on the other side, when z_l is reduced, it should be energetically easier to disorder the local magnetic moments by flipping or canting them. If the latter effect dominates, the Curie temperature would tend to decrease with decreasing coordination.

In order to derive reliable conclusions concerning the environmental dependence of the magnetization curves and Curie temperatures, one requires an electronic theory that takes into account both the fluctuations of the magnetic moments and the itinerant character of the *d* electron states. Simple spin Hamiltonians, for example based on the Heisenberg, *xy* or Ising models, are not expected to be very predictive, at least until they incorporate the electronic effects responsible for the environmental dependence of the interactions between the magnetic moments.

The electronic structure calculations based on density functional theory or realistic model Hamiltonians have been very successful in describing a wide variety of experimental results on the magnetic properties of low-dimensional systems and nanostructures, particularly concerning the spin moments, orbital moments, and magnetic anisotropy at low temperatures.[1,2,26] In contrast, a detailed understanding of the magnetism of TM nanostructures at finite temperature remains an open problem.[14,15,17–21] Most of the studies so far have been performed by means of *k*-space approaches[14] or simplified model Hamiltonians.[15,17,20] For instance, Razee *et al.* calculated the Curie temperature of Fe and Co films as a function of thickness by using a method that separates spin fluctuations from electronic hoppings on the basis of their different characteristic times.[14] The relevant spin excitations are treated as classical spins by taking into account the changes in the orientation of the magnetic moments. Wu *et al.* studied the magnetic reorientation transitions in thin films by using a modified alloy analogy in the framework of the single-band Hubbard Hamiltonian.[20] In addition, Pajda *et al.* showed that it is necessary to go beyond mean-field approximations in order to obtain the correct Curie temperature in systems with a large susceptibility to fluctuations.[18] Besides these findings, the theoretical description of systems having a

reduced dimensionality and symmetry remains a major challenge. One of the central issues is to understand the correlation between the temperature dependence of the magnetic behavior and the parameters that characterize the morphology and composition of the system, which can be controlled in experiment. This concerns properties such as the Curie temperature, the critical exponents characterizing $M(T)$, as well as possible changes in the nature of the relevant spin excitations as a function of dimensionality.

The purpose of this paper is to investigate the interplay between local environment and the stability of ferromagnetism at finite temperatures by determining the local magnetization curves $M_l(T)$ and spin fluctuation energies of ultrathin Fe films. In Sec. II we present the method used for the calculations, which is based on Hubbard and Hasegawa's spin fluctuation theory for the periodic solid,[27,28] as recently extended in the context of cluster magnetism.[29] The temperature dependence of the local moments, layer magnetizations $M_l(T)$, and spin fluctuation energies of ultrathin bcc (001) films is presented and discussed in Sec. III. Comparison is made with the corresponding bulk results in order to quantify the role of dimensionality. Strain and local environmental effects are quantified by varying the interatomic distances d. Finally, Sec. IV summarizes the main conclusions by pointing out goals, limitations, and some possible extensions.

II. THEORY

In the following we present the functional-integral theory used for the calculations of the magnetic properties of TM films.[29] For simplicity, we consider a d-band Hamiltonian since the magnetic properties of the transition metals are dominated by the $3d$-electron states. For instance, the contribution of s- and p-electrons to the spin magnetic moment is less than 4%.[30,31] This is mainly a consequence of the much stronger Coulomb interactions and higher density of states of the d electrons, as compared to the s and p states. Moreover, notice that the contribution of the sp electrons and sp-d hybridizations to the itinerant nature of the d states is taken into account effectively in our model through the d-band filling and bandwidth, which do not depend strongly on temperature in the relevant range. Consequently, it is a very good approximation to consider only the d electrons when computing the temperature dependence of the magnetization. The d-electron Hamiltonian is written as[25]

$$\hat{H} = \hat{H}_0 + \hat{H}_I. \tag{1}$$

The first term

$$\hat{H}_0 = \sum_{l,\alpha,\sigma} \varepsilon_l^0 \hat{n}_{l\alpha\sigma} + \sum_{\substack{l\neq m \\ \alpha,\beta,\sigma}} t_{lm}^{\alpha\beta} \hat{c}_{l\alpha\sigma}^{\dagger} \hat{c}_{m\beta\sigma} \tag{2}$$

describes the single-particle electronic structure of the valence d electrons in the tight-binding approximation.[32] As usual, $\hat{c}_{l\alpha\sigma}^{\dagger}$ ($\hat{c}_{l\alpha\sigma}$) refers to the creation (annihilation) operator of an electron with spin σ at the orbital α of atom l ($\alpha \equiv xy$, yz, zx, x^2-y^2, and $3z^2-r^2$), and $\hat{n}_{l\alpha\sigma}=\hat{c}_{l\alpha\sigma}^{\dagger}\hat{c}_{l\alpha\sigma}$ is the corresponding number operator. ε_l^0 stands for the bare d-level energy of the isolated atom and $t_{lm}^{\alpha\beta}$ for the hopping integrals between atoms l and m. The second term

$$\hat{H}_I = \frac{1}{2} \sum_{\substack{l,\alpha,\beta \\ \sigma,\sigma'}}{}' U_{\sigma\sigma'} \hat{n}_{l\alpha\sigma} \hat{n}_{l\beta\sigma'} \tag{3}$$

approximates the interactions among electrons by an intra-atomic Hubbard-like model. The Coulomb repulsions $U_{\sigma\sigma'}$ between electrons of spin σ and σ' are the average direct Coulomb integral $U_{\uparrow\downarrow}=U_{\downarrow\uparrow}=F^{(0)}$ and $U_{\uparrow\uparrow}=U_{\downarrow\downarrow}=U_{\uparrow\downarrow}-J$, where $J=(F^{(2)}+F^{(4)})/14$ refers to the average exchange integral. The $F^{(i)}$ with $i=0$, 2, and 4 stand for the radial d-electron Coulomb integrals allowed by atomic symmetry.[33] These are obtained by taking the ratios $F^{(0)}/F^{(2)}$ and $F^{(4)}/F^{(2)}$ from atomic calculations[34] and by fitting the value of $F^{(2)}$ to reproduce the bulk Fe spin moment at zero temperature. Notice that Eq. (3) does not respect spin-rotational symmetry since the exchange terms of the form $H_{xy}=-\Sigma_{l,\alpha<\beta}J_{\alpha\beta}(S_{l\alpha}^{-}S_{l\beta}^{+}+S_{l\alpha}^{+}S_{l\beta}^{-})$ have been dropped.[35] Nevertheless, this is not expected to be a serious limitation in the present work because we are interested in studying the spin fluctuations on top of broken-symmetry ferromagnetic ground states.

A. Partition function and thermodynamic properties

The finite temperature properties are determined by applying the functional-integral formalism developed by Hubbard and Hasegawa for periodic solids.[27,28] The many-body interaction can be written as

$$\hat{H}_I = \sum_l \left(\frac{U}{2} \hat{N}_l^2 - J \hat{S}_{lz}^2 \right), \tag{4}$$

where $\hat{N}_l=\Sigma_{\alpha\sigma}\hat{n}_{l\alpha\sigma}$ is the electron number operator at atom l, and $\hat{S}_{lz}=(1/2)\Sigma_{\alpha}(\hat{n}_{l\alpha\uparrow}-\hat{n}_{l\alpha\downarrow})$ is the z component of the spin operator. $U=(U_{\uparrow\downarrow}+U_{\uparrow\uparrow})/2$ represents an average direct Coulomb repulsion. Notice that Eq. (4) includes the self-interaction terms $U_{\uparrow\uparrow}\hat{n}_{l\alpha\sigma}^2/2=U_{\uparrow\uparrow}\hat{n}_{l\alpha\sigma}/2$ which are canceled out by redefining the d-energy levels as $\varepsilon_l^0-U_{\uparrow\uparrow}/2$. For the calculation of the partition function Z, the quadratic terms in Eq. (4) are linearized by means of a two-field Hubbard-Stratonovich transformation within the static approximation. This corresponds to decoupling the electronic hoppings from the relatively slower spin fluctuations. A charge field η_l and an exchange field ξ_l are introduced at each site l, which represent the local finite-temperature fluctuations of the d-electron energy levels and exchange splittings, respectively. Using the notation $\vec{\xi}=(\xi_1,\ldots,\xi_n)$ and $\vec{\eta}=(\eta_1,\ldots,\eta_n)$ for an n-sites system, Z is given by

$$Z \propto \int d\vec{\eta} d\vec{\xi} Z'(\vec{\xi},\vec{\eta}), \tag{5}$$

where

$$Z'(\vec{\xi},\vec{\eta}) = \exp\{-\beta F(\vec{\xi},\vec{\eta})\} \tag{6}$$

$$=\exp\left\{-\frac{\beta}{2}\sum_l\left[U\eta_l^2+\frac{J}{2}\xi_l^2\right]\right\}\times \mathrm{Tr}[\exp\{-\beta(\hat{H}'-\mu\hat{N})\}]. \tag{7}$$

$F(\vec{\xi},\vec{\eta})$ can be regarded as a free energy which depends on the fields $\vec{\xi}$ and $\vec{\eta}$. The static approximation is exact in the atomic limit ($t_{lm}^{\alpha\beta}=0,\ \forall l\neq m$) where no fluctuations are present, and in the noninteracting limit ($U_{\sigma\sigma'}=0$). For nontrivial cases $\hat{H}'$ describes the dynamics of the d electrons as if they were independent particles moving in a random alloy with energy levels $\varepsilon'_{l\sigma}$ given by

$$\varepsilon'_{l\sigma}=\varepsilon_l^0+Ui\,\eta_l-\sigma\frac{J}{2}\xi_l. \tag{8}$$

The thermodynamic properties of the system are obtained as a statistical average over all possible distributions of the energy levels $\varepsilon'_{l\sigma}$ throughout the system. From Eqs. (6) and (7) one obtains

$$\frac{\partial F(\vec{\xi},\vec{\eta})}{\partial\xi_l}=\frac{J}{2}(\xi_l-2\langle\hat{S}_{lz}\rangle'_{\vec{\xi},\vec{\eta}}) \tag{9}$$

and

$$\frac{\partial F(\vec{\xi},\vec{\eta})}{\partial\eta_l}=U(\eta_l+i\langle\hat{N}_l\rangle'_{\vec{\xi},\vec{\eta}}), \tag{10}$$

where

$$\langle\hat{N}_l\rangle'_{\vec{\xi},\vec{\eta}}=\int_{-\infty}^{+\infty}\sum_{\alpha\sigma}\rho_{l\alpha\sigma}(\varepsilon)f(\varepsilon)d\varepsilon \tag{11}$$

and

$$2\langle\hat{S}_l\rangle'_{\vec{\xi},\vec{\eta}}=\int_{-\infty}^{+\infty}\sum_{\alpha\sigma}\sigma\rho_{l\alpha\sigma}(\varepsilon)f(\varepsilon)d\varepsilon. \tag{12}$$

Here, $\langle\cdots\rangle'$ indicates average with respect to the single-particle Hamiltonian H', $f(\varepsilon)$ refers to the Fermi function, and $\rho_{l\alpha\sigma}(\varepsilon)$ to the local density of states (DOS) at the orbital $l\alpha\sigma$.[29] Notice that by setting Eqs. (9) and (10) equal to zero one recovers the usual self-consistent mean-field equations for η_l and ξ_l at $T=0$.[25] The present formulation is therefore a natural extension of a widely used ground-state mean-field approach.

Since we are mainly interested in the magnetic properties and since $J\ll U$, we neglect the thermal fluctuations of the charge fields η_l by setting them equal to the exchange-field-dependent saddle-point values $i\,\eta_l=\nu_l=\langle\hat{N}_l\rangle'_{\vec{\xi}}$. This amounts to a self-consistent determination of the charge distribution for each exchange-field configuration $\vec{\xi}$. In this way

$$Z\propto\int d\vec{\xi}\,\tilde{Z}'(\vec{\xi}), \tag{13}$$

where

$$Z'(\vec{\xi})=\exp\{-\beta F(\vec{\xi})\} \tag{14}$$

$$=\exp\left\{\frac{\beta}{2}\sum_l\left[U\nu_l^2-\frac{J}{2}\xi_l^2\right]\right\}\times \mathrm{Tr}[\exp\{-\beta(\hat{H}'-\mu\hat{N})\}] \tag{15}$$

depends now only on the exchange variables $\vec{\xi}$ that describe the relevant fluctuations of the spin degrees of freedom. Thus $F(\vec{\xi})$ represents the free energy associated to the exchange-field configuration $\vec{\xi}$.[36]

The integrand $\exp\{-\beta F(\vec{\xi})\}$ is interpreted as proportional to the probability $P(\vec{\xi})$ for a given exchange-field configuration $\vec{\xi}$. The thermodynamic properties are obtained by averaging over all possible $\vec{\xi}$ with $\exp\{-\beta F(\vec{\xi})\}$ as weighting factor. For example, the local magnetization at atom l is given by

$$M_l(T)=\frac{1}{Z}\int d\vec{\xi}\exp\left\{\frac{\beta}{2}\sum_l\left(U\nu_l^2-\frac{J}{2}\xi_l^2\right)\right\}\times\mathrm{Tr}[2\hat{S}_l^z\exp\{-\beta(\hat{H}'-\mu\hat{N})\}] \tag{16}$$

$$=\frac{1}{Z}\int d\vec{\xi}\,2\langle S_{lz}\rangle'_{\vec{\xi}}e^{-\beta F'(\vec{\xi})}, \tag{17}$$

where $\langle S_{lz}\rangle'_{\vec{\xi}}$ is the average spin moment corresponding to the effective single-particle Hamiltonian H' which depends on the fluctuating $\vec{\xi}$. Taking into account that $\partial F/\partial\xi_l=J(\xi_l-2\langle\hat{S}_{lz}\rangle'_{\vec{\xi}})/2$ and integrating Eq. (17) by parts one obtains

$$M_l(T)=\int\xi_l P_l(\xi)d\xi, \tag{18}$$

where we have introduced the probability

$$P_l(\xi)=\frac{1}{Z}\exp\{-\beta F_l(\xi)\} \tag{19}$$

$$=\frac{1}{Z}\int\prod_{m\neq l}d\xi_m\exp\{-\beta F(\xi_1,\ldots,\xi_{l-1},\xi,\xi_{l+1},\ldots,\xi_n)\}. \tag{20}$$

Thus the temperature dependent local magnetization is equal to the average of the local exchange field. Equation (18) justifies the intuitive association between the fluctuations of the local moment $2\langle\hat{S}_{lz}\rangle$ at atom l and those of the exchange field ξ_l. Besides the local magnetizations $M_l(T)$ it is interesting to compute the average module of the local moments μ_l which are given by

$$\mu_l=2\sqrt{\langle\hat{S}_{lz}^2\rangle}=\left[-\frac{2}{\beta J}+\int\xi_l^2P_l(\xi_l)d\xi_l\right]^{1/2}. \tag{21}$$

As in the case of M_l, μ_l is given by a statistical average over the probability distribution $P_l(\xi)$.

B. Alloy analogy approximation

Equations (18)–(21) show that the magnetic properties at finite temperature can be determined in a similar way as in

an alloy where the energy levels depend on the configuration of the exchange fields $\vec{\xi}$, which occurs with a probability $P(\vec{\xi})$. The simplest method for calculating alloy averages is the single-site virtual crystal approximation (VCA). For each layer l one determines the local Green's function assuming that the site l is embedded in an effective medium characterized by the average of the energy levels.[37] The effective medium is characterized by the Hamiltonian $\hat{H}_{\text{eff}}=\hat{H}_0+\langle\hat{H}'_l\rangle$ and its corresponding Green's function $\hat{G}_{\text{eff}}(\varepsilon)$. $\hat{H}_{\text{eff}}$ depends on the average values $\langle\nu_l\rangle$ and $\langle\xi_l\rangle$ which are calculated self-consistently by taking into account the fluctuations of ξ at site l. The free energy is obtained by integrating

$$\frac{\partial F(\xi_l)}{\partial \xi_l}=\frac{J}{2}(\xi_l-2\langle\hat{S}_{lz}\rangle_{\xi_l}). \tag{22}$$

The average spin moments $\langle\hat{S}_{lz}\rangle_{\xi_l}$ are calculated from Eq. (12) where $\rho_{l\alpha\sigma}$ is the local DOS at site l having an exchange field ξ_l embedded in the average effective medium. The perturbed Hamiltonian $\hat{H}_{\text{p}}$ is then given by

$$\hat{H}_{\text{p}}=\hat{H}_{\text{eff}}+\hat{V}_l, \tag{23}$$

where

$$\hat{V}_l=\sum_{\alpha\sigma}[U(\nu_l-\langle\nu_l\rangle)-\sigma J/2(\xi_l-\langle\xi_l\rangle)]\hat{n}_{l\alpha\sigma}. \tag{24}$$

Finally, the local Green's function at site l, from which $\rho_{l\alpha\sigma}$ is derived, is obtained using the Dyson equation.

A more accurate though numerically more involved description of disorder is obtained with the coherent potential approximation (CPA) which treats scattering effects self-consistently. In the CPA the effective medium is characterized by a complex self-energy $\hat{\Sigma}(\varepsilon)$ that matches self-consistently (for each energy ε) the average of the perturbed Green's function associated to ξ_l and the Green's function $\hat{G}_{\text{eff}}$ of the surrounding medium.[37] The effective Hamiltonian is written as $\hat{H}_{\text{eff}}=\hat{H}_0+\hat{\Sigma}$, and the perturbed Hamiltonian is given by Eq. (23) with the perturbation

$$\hat{V}_l=\sum_{\alpha\sigma}(U\nu_l-\sigma J/2\xi_l)\hat{n}_{l\alpha\sigma}-\hat{\Sigma}_l. \tag{25}$$

Finally, the self-consistent equation for the self-energy reads

$$\hat{\Sigma}_l=\langle[\hat{\mathbb{1}}_l-\hat{G}_{l\,\text{eff}}\hat{V}_l]^{-1}(\hat{V}_l+\hat{\Sigma}_l)\rangle. \tag{26}$$

Notice that the probability distribution of the exchange fields is determined self-consistently. As in the VCA, the free energy $F(\xi_l)$ is calculated by integrating Eq. (22) and the local DOS in Eq. (12) are obtained by applying the Dyson equation.

III. RESULTS

The parameters used for the calculations on Fe bulk and films are the same as in Ref. 25, namely, bulk d-band width $W=6.0$ eV, direct Coulomb integral $U=6.0$ eV, and exchange integral $J=0.70$ eV, which reproduce the bulk spin moment $\mu_b=2.21\ \mu_{\text{B}}$ at $T=0$. The Green's functions of the effective medium are computed by using Haydock-Heine-Kelly's recursion method.[38] In the following sections we present and discuss our results for bulk bcc Fe and for (001) ultrathin films. The calculations are performed by using the VCA and the CPA. It is of considerable interest to compare the VCA results with the more accurate self-consistent CPA. In fact, comparing VCA and CPA gives some insight on the effects of the disorder induced by the spin fluctuations on the electronic structure and on the resulting magnetization curves. Moreover, the simplicity of the VCA makes it an attractive tool to explore complex low-symmetry nanostructures.

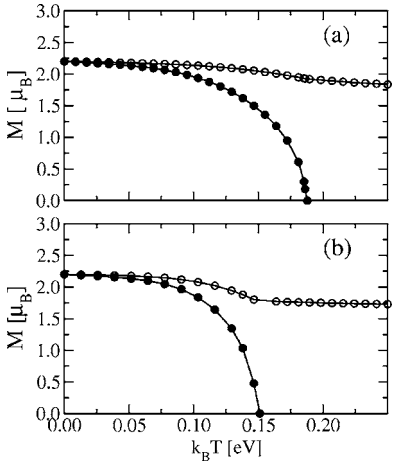

FIG. 1. Temperature dependence of the magnetization M for bulk bcc Fe (dots) as obtained by using (a) the VCA and (b) the CPA. The open circles are the corresponding local magnetic moment as given by Eq. (21).

A. Fe bulk

In order to quantify the effects of reduced dimensionality and as a reference for further discussion, it is useful to consider the case of the periodic solid in some detail. The temperature dependence of the magnetization $M_{l_z}(T)$ and of the local magnetic moment $2\sqrt{\langle\hat{S}_{lz}^2\rangle}$ of bulk Fe are shown in Fig. 1. Figures 1(a) and 1(b) refer to calculations by using the VCA and the CPA, respectively. First of all, one observes that the temperature dependence of $M_l(T)$ is qualitatively similar to the experimental one. Notice that for $T>T_C$ we find nonvanishing $2\sqrt{\langle\hat{S}_{lz}^2\rangle}$ with a weak temperature dependence, which agrees with previous calculations.[39] Moreover, the values obtained for T_C are close to those found in recent first principles calculations.[13] However, notice that the calculated T_C is appreciably larger than the experimental value $T_C^{\text{exp}}=1043$ K. The effects of additional spin excitations like spin-waves, short-range order, possible noncollinear spin moments, and correlations beyond the static approximation[40] should tend to reduce T_C and improve the quantitative agreement.

It is interesting to observe that the VCA and the CPA yield similar behaviors. Moreover, the VCA and CPA results are in

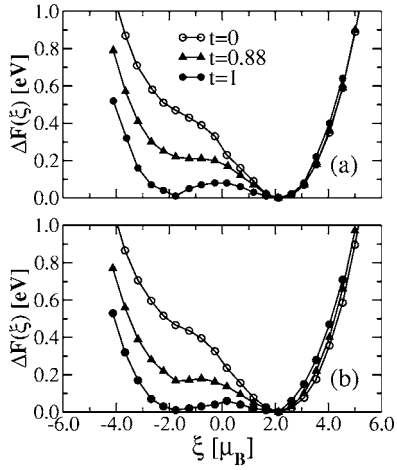

FIG. 2. Local spin-fluctuation energy $\Delta F(\xi)=F(\xi)-F(\xi^{0+})$ in bulk bcc Fe, where $F(\xi^{0+})$ refers to the minimum of the free energy for $\xi>0$. The average of spin fluctuations in the surrounding medium is performed using (a) the VCA and (b) the CPA. The considered reduced temperatures $t=T/T_C$ are indicated in the inset.

qualitative agreement with the main trends observed in experiment and in previous calculations using *ab initio* methods and dynamical mean field theory.[13] However, there are two main differences that deserve to be mentioned. First, in the VCA, the form of $M_l(T)$ for $T\rightarrow T_C$ approaches zero more slowly and in general $2\sqrt{\langle \hat{S}_{lz}^2\rangle}$ is larger than in the CPA. Second, the value of T_C is about 15% smaller in the CPA than in the VCA. This can be understood by recalling that the VCA works best in the dilute limit (i.e., $T\rightarrow 0$). As the temperature increases, the negative exchange-fields are not taken properly into account by the average effective medium. This results in an overestimation of T_C as compared to the CPA which takes into account large spin fluctuations more accurately close to the critical point.[37] However, it is important to remark that for $T\rightarrow T_C$ both approximations fail to describe the correct critical behavior of the phase transition since the present single-site alloy analogy does not correctly describe the long range fluctuations of the order parameter.

In order to complete the discussion of bulk Fe we show in Fig. 2 the average local spin fluctuation energy $\Delta F(\xi)$ as a function of ξ. The average over spin fluctuations in the surrounding medium is performed using the VCA and the CPA. The temperature dependence of $\Delta F(\xi)$ is illustrated by considering three representative reduced temperatures $t=T/T_C=0$, 0.88, and 1. At $T=0$ one observes a single well-defined minimum at $\xi=\xi^{0+}>0$ and an inflexion point at $\xi=\xi^{0-}<0$ with $|\xi^{0-}|<\xi^{0+}$. As T increases and approaches T_C, a second minimum starts to develop out of the saddle point at ξ^{0-} and at the same time one observes a small decrease of ξ^{0-} (see Fig. 2). Finally, for $T\geqslant T_C$, $\Delta F(\xi)$ becomes symmetric, showing that the positive and negative ξ occur with the same probability. The Curie temperature can be regarded as the temperature at which it costs no free energy to flip an exchange field. A similar behavior has been obtained in previous studies.[27] It is interesting to observe that the VCA and the CPA yield very similar results, which suggests that in first approximation $\Delta F(\xi)$ is dominated by local effects. Notice

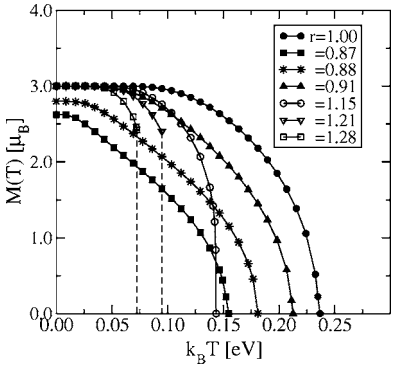

FIG. 3. Temperature dependence of the magnetization of a (001) Fe monolayer calculated by using the VCA. Results are given for several values of the nearest-neighbor bond length d ($r=d/d_{\mathrm{bulk}}$).

that the energy barrier between the two minima at $T\simeq T_C$ is appreciably smaller than k_BT_C [e.g., in the VCA $F(0)-F(\xi^{0+})\simeq 0.08$ eV for $k_BT=k_BT_C^{\mathrm{VCA}}=0.18$ eV]. One concludes that in bulk Fe not only the changes of sign of ξ around ξ^{0+} and ξ^{0-} but also the fluctuations of the size of the exchange splittings are very important at finite T. This behavior is a characteristic of itinerant magnetism which contrasts with the simpler fluctuations of the direction of localized magnetic moments. As it will be discussed below, low dimensional systems and in particular ultrathin films show a somewhat different behavior with a stronger tendency to favor localized spin excitations.[29]

B. Fe thin films

In this section, we consider a bcc (001) monolayer and a five-layer Fe film as representative examples of low dimensional systems. The interplay between local environment and magnetic properties is investigated by varying the NN distances around the values corresponding to the bulk and to some relevant substrates.

Figure 3 shows the VCA results for $M_l(T)$ for several values of $r=d/d_{\mathrm{bulk}}$. Starting from small values of r we observe an increase of the ground-state magnetization $M_l(0)$ with increasing r up to the saturated value $M_l(0)=(10-n_d)$. This is due to the narrowing of the d band with increasing NN distance. As it will be discussed below, the changes of $M_l(0)$ play an important role on the behavior of $M_l(T)$ as a function of r. Notice that for $0.92<r<1$ the temperature dependence of the magnetization in the monolayer follows qualitatively the same form as in the bulk (see Fig. 1). However, for small r ($r<0.88$), the decrease of the magnetization with temperature becomes almost linear for intermediate T. This indicates that the spin-flip excitations are more likely to occur, since the magnetic moments are smaller (see Fig. 3 for $r=0.866$). On the other side, for large values of r ($r>1.15$), the more localized character of the electrons allows strong spin fluctuations only close to T_C. This changes the form of $M_l(T)$ with respect to the case $0.86<r<1$ (see Fig. 3).

The results obtained for the monolayer within the CPA show several main trends in common with the VCA (see Figs. 3 and 4). However, comparison with the bulk results

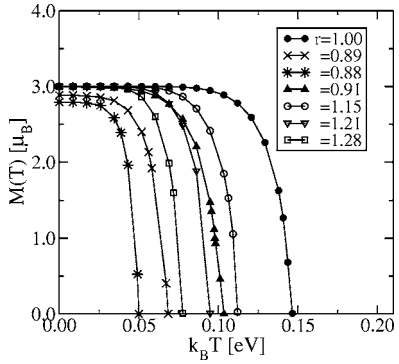

FIG. 4. Temperature dependence of the magnetization of a (001) Fe monolayer calculated by using CPA. Results are given for several values of the nearest-neighbor bond length d ($r=d/d_{\mathrm{bulk}}$).

discussed in the previous section reveals a remarkable quantitative difference. In the bulk, the CPA yields a T_C about 15% smaller than the one obtained with the VCA, while in the case of the monolayer this reduction is about 35%. This is related to the changes in the nature of the spin excitations as the coordination number decreases. As it will be discussed below, in the monolayer the dominant spin fluctuations are changes of sign of ξ so that the probability distribution $P(\xi)$ resembles a binary alloy. In this case the limitations of the VCA are known to be relatively important. One concludes that the VCA becomes less accurate as the dimensionality decreases.

In order to provide further physical insight into the behavior of $M_l(T)$ for the (001) monolayer, we show in Fig. 5 the spin-fluctuation energies $\Delta F(\xi_l)=F(\xi_l)-F(\xi_l^{0+})$ calculated in the VCA, where ξ_l^{0+} indicates the position of the minimum of the free energy for $\xi_l>0$. Results are given for several representative temperatures T and NN distances. One observes for all the curves a two minima structure with a well-defined second minimum at $\xi_l^0<0$. In contrast, the $T=0$ bulk curve displays only an inflexion point in the same range of $\xi<0$. This indicates that in the monolayer the spin-flip excitations (changes of sign of ξ) are likely to occur even at relatively low T. Consequently, one finds a binarylike distribution for all the considered NN distances. In addition, let us recall as already shown in Fig. 3 that the largest Curie temperature is found for $r=d/d_{\mathrm{bulk}}=1$. This is consistent with the fact that for $r=1$ the spin-flip energies are the largest, e.g., $\Delta F_{\pm}=F(\xi_l^{0+})-F(\xi_l^{0-})\simeq 0.75$ eV at $T=0$ (see Fig. 5). Once the fluctuation effects become important ($t\approx 0.9$), $\Delta F_{\pm}(0)$ decreases rapidly, with increasing T and vanishes at the Curie temperature. It is also interesting to notice that the larger T_C is, the slower the spin-flip energy changes with temperature (see Fig. 5). This reinforces the physical picture that the Curie temperature is not given by the energy necessary to flip a spin at $T=0$ but it is rather the temperature at which it costs no free-energy to flip one.

As r decreases, e.g., for $r=0.881$ and 0.866 in Figs. 5(c) and 5(d), the dependence of $\Delta F_{\pm}(T)$ with temperature changes. For $r=0.881$ and 0.866, $\Delta F_{\pm}(T)$ increases in the low temperature range ($t\lesssim 0.55$), while for high values of $t(t\gtrsim 0.9)$, $\Delta F_{\pm}(T)$ decreases. This implies that for $r=0.881$ and 0.866 there is a tendency to favor negative values of ξ

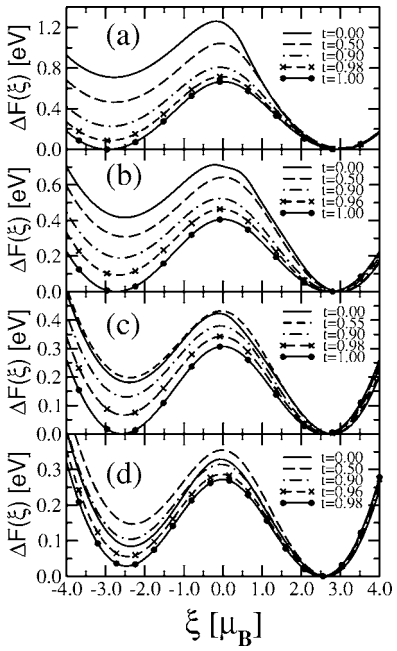

FIG. 5. Local spin-fluctuation energy $\Delta F(\xi_l)=F(\xi_l)-F(\xi_l^{0+})$ in a bcc (001) Fe monolayer with different NN distances d: (a) $r=d/d_{\mathrm{b}}=1$, (b) $r=0.91$, (c) $r=0.88$, and (d) $r=0.87$. $F(\xi_l^{0+})$ refers to the minimum of the free energy $\xi>0$. The considered reduced temperatures $t=T/T_C$ are indicated in the inset. The VCA is used for the average of spin fluctuations in the surrounding medium.

(even at low T). Rather than a finite temperature effect, this is mainly related to the electronic structure.

It is interesting to contrast the role of the local environment on the ground state and finite temperature properties and to establish correlations between them. For this purpose we present in Fig. 6 the VCA and CPA results for the magnetization $M_l(0)$ at $T=0$ and for the Curie temperature T_C as a function of the nearest-neighbor distance d. In this way the interplay between kinetic and Coulomb energies can be explored, since shorter NN distances yield larger d-band widths which correspond to larger coordination numbers. One first observes that the ground-state moment grows rapidly with increasing d as the density of states as the Fermi energy increases (Stoner criterion). At some point $M_l(0)$ reaches the saturation value $M_{\mathrm{sat}}=10-n_d$ beyond which $M_l(0)$ is independent of d. The Curie temperature, which measures the stability of ferromagnetism at finite T, shows a much more interesting nonmonotonous behavior that can be qualitatively interpreted in terms of a mean-field Heisenberg model for the atomic spins. In this framework $k_{\mathbf{B}}T_C\simeq zJ_{\mathrm{H}}M_l(0)^2/3$, where z is the coordination number, J_{H} is the effective Heisenberg coupling between NN spins, and $M_l(0)$ is the $T=0$ moment. Three different regimes can be distinguished. First, for $0.866\leqslant d/d_{\mathrm{b}}\leqslant 0.912$ T_C increases due to the increase of the local moments and the associated enhancement of the exchange splitting $\Delta\varepsilon_x^d$ [see Figs. 6(a) and 6(b)]. In this range $M_l(0)$ and $\Delta\varepsilon_x^d$ increase significantly, which dominates over the effects of the reduction of the NN hoppings on the magnetic order. In fact the effective Heisenberg coupling $J_{\mathrm{H}}\simeq 3k_BT_C/[zM_l(0)^2]$ increases with d, for example, in the CPA, from $J_{\mathrm{H}}\simeq 4.5$ meV$/\mu_{\mathrm{B}}^2$ for $d/d_{\mathrm{bulk}}=0.88$ to J_{H}

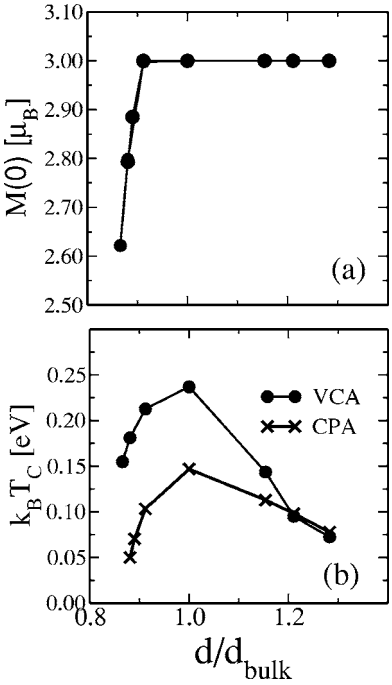

FIG. 6. (a) Ground-state magnetization $M_l(0)$ and (b) Curie temperature T_C of a bcc (001) Fe monolayer as a function of the nearest-neighbor distance d. Dots (crosses) refer to VCA (CPA) results.

$\simeq 8.3$ meV/μ_B^2 for $d/d_{\text{bulk}}=0.91$. The subtle effects of itinerant magnetism become even more evident for $0.9<d/d_{\text{bulk}} \leqslant 1$ where $M_l(0)$ is constant and still T_C increases. Notice that in this range the mean-field exchange splitting at $T=0$ is also constant so that the enhancement of T_C must be ascribed to changes in the electronic structure in the presence of spin fluctuations (random alloy). Finally, for $d/d_{\text{bulk}}>1$ the behavior changes and the effective J_H decreases with increasing d. In this case the electronic hoppings and the kinetic energy of the electrons are small and the spin fluctuations have a more localized character. Consequently, as d increases the spin-fluctuation energies decrease, since the perturbations introduced by disorder are less significant. In summary, the distance dependence of the finite-temperature properties are the result of a subtle competition between localized and itinerant aspects of magnetism. Interesting phenomena can also be expected as a function of other variables such as the local coordination number which affects the relative importance of kinetic and Coulomb contributions.

The geometry of thicker films introduces very interesting additional effects resulting from the interaction between magnetic moments in different local environments. As a representative example we consider in Fig. 7 the layer-resolved magnetization curves $M_l(T)$ of a five-layer bcc (001) Fe film in the VCA. For the sake of comparison the corresponding bulk magnetization curve is also shown. The temperature dependence of $M_l(T)$ at the surface layers is quite different from that of the inner layers. At low temperatures the surface shows a rapid linear decrease of $M_1(T)$ which indicates that the spin-fluctuation energies are lower despite the larger ground-state moments. A similar linear decrease of $M(T)$ has

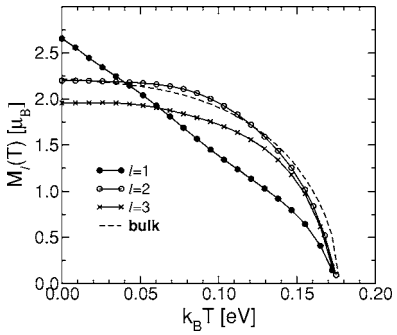

FIG. 7. Layer magnetization $M_l(T)$ of a five-layer bcc (001) Fe film in the VCA. $l=1$ (dots) refers to the surface layers, $l=2$ (open circles) to the layers below the surface, and $l=3$ (crosses) to the central layer. The dashed curve shows the corresponding bulk results.

been found in experiments[10,11] and calculations[16] on Fe surfaces. In contrast, the form of $M_l(T)$ and the local moments at $T=0$ of the inner layers ($l=2$ and 3) are similar to those of the bulk. One actually observes that $M_l(T)$ for $l=2$ and 3 scales with the ground moment $M_l(0)$. This is not the case for $l=1$. The surface-layer magnetization curve is similar to the one found for a free-standing monolayer but having a shorter interatomic distance $d/d_{\text{bulk}}=0.87$. In this case, the ground-state moment is enhanced with respect to the bulk by a comparable amount as it is found at the surface of the five-layer film (see Fig. 3). Let us recall that in the monolayer with $d/d_{\text{bulk}}=0.87$ the reduction of the spin-fluctuation energies dominates in front of the enhancement of the local moments, both consequences of the reduction of z, thus yielding a smaller T_C than in the bulk.

The contributions of the inner layers dominate the magnetic behavior of the film as a whole. In fact, the Curie temperature of the five-layer film is only 5% lower that the bulk one. This appears to be the result of compensation between the contributions of surface and inner layers. On the one side, the surface layers show a very rapid decrease of $M_1(T)$ that seems to point to a T_C smaller than the bulk. And on the other side, the ferromagnetic order is more stable at the inner layers which have a complete NN shell ($l=2$ and 3). In particular close to T_C, the coupling between inner and surface layers tends to stabilize the magnetization in the latter.

IV. CONCLUSION

The finite-temperature magnetic properties of bulk Fe and of ultrathin Fe films have been determined in the framework of a functional-integral itinerant-electron theory. The effects of disorder due to spin fluctuations have been taken into account by considering two different approaches, namely, the virtual crystal and coherent potential approximations. The stability of ferromagnetism has been studied as a function of the local environment of the atoms. A remarkable nonmonotonous dependence of the magnetization curves has been obtained by varying the interatomic distances (strain effects) and by considering different positions of the atoms within the film (layer dependence). Moreover, the reduction of the

system dimensions, from 3D to 2D, enhances the localized character of the spin fluctuations. These trends have been correlated with the environmental dependence of the electronic properties and with the resulting changes in the ground-state magnetic moments and spin-fluctuation energies. The electronic structure contributions and the itinerant character of the *d* electrons are crucial for determining the magnetic behavior of low-dimensional systems at finite temperatures.

Several important aspects of the problem still remain to be addressed. The magnetic properties of TM nanostructures are conditioned by the interplay between kinetic and Coulomb energies. The former is responsible for electron delocalization and band formation, as well as for the coupling between the spins at different atoms, while the latter is the driving force stabilizing the formation of local magnetic moments. Therefore the relative importance of these two contributions depends strongly on the system geometry and on the local atomic environment. The present electronic model and the local approach to the electronic structure are well-suited to investigate more complex systems with reduced symmetry, such as clusters and nanostructures on surfaces or substrate effects on thin films. Moreover, a number of methodological improvements are worthwhile. For instance, noncollinear magnetic order and fluctuations of the exchange fields are likely to affect the magnetization curves and probably reduce the calculated value of T_C. The effects of interfaces with nonmagnetic substrates should be incorporated in order to achieve a more realistic comparison with experiment. In addition the model can be readily extended to take into account spin-orbit interactions,[26] and dipole-dipole interactions which are responsible for the magnetic anisotropy and for the spin reorientation transitions as a function of temperature and structure.[8,9,41,42] Finally, it remains a major challenge to improve on the treatment of many-body effects beyond the static approximation, since the electronic correlations are expected to become increasingly important as the system dimension decreases.

ACKNOWLEDGMENTS

This work was supported in part by CONACyT Mexico (Grant No. 39517). R.G.A. acknowledges PIFOP 2002-26-01. Computer resources were provided by IDRIS (CNRS, France).

[1] L. M. Falicov, D. T. Pierce, S. D. Bader, R. Gronsky, K. H. Hathaway, H. J. Hopster, D. N. Lambeth, S. S. P. Parkin, G. Prinz, M. Salamon, I. K. Schuller, and R. H. Victora, J. Mater. Res. **5**, 1299 (1990); M. T. Johnson, P. J. H. Bloemen, F. J. A. den Broeder, and J. J. de Vries, Rep. Prog. Phys. **59**, 15409 (1996); J. Shen and J. Kirschner, Surf. Sci. **500**, 300 (2002).

[2] J. Bansmann, S. H. Baker, C. Binns, J. A. Blackman, J.-P. Bucher, J. Dorantes-Dávila, V. Dupuis, L. Favre, D. Kechrakos, A. Kleibert, K.-H. Meiwes-Broer, G. M. Pastor, A. Perez, O. Toulemonde, K. N. Trohidou, J. Tuaillon, and Y. Xie, Surf. Sci. Rep. **56**, 189 (2005).

[3] A. Lisfi, J. C. Lodder, H. Wormeester, and B. Poelsema, Phys. Rev. B **66**, 174420 (2002); J. Langer, J. H. Dunn, A. Hahlin, O. Karis, R. Sellmann, D. Arvanitis, and H. Maletta, *ibid.* **66**, 172401 (2002); H. J. Choi, W. L. Ling, A. Scholl, J. H. Wolfe, U. Bovensiepen, F. Toyama, and Z. Q. Qiu, *ibid.* **66**, 014409 (2002).

[4] S. Förster, G. Baum, M. Müller, and H. Steidl, Phys. Rev. B **66**, 134427 (2002); G. Gubbiotti, G. Carlotti, M. G. Pini, P. Politi, A. Rettori, P. Vavassori, M. Ciria, and R. C. O'Handley, *ibid.* **65**, 214420 (2002); R. Vollmer, S. van Dijken, M. Schleberger, and J. Kirschner, *ibid.* **61**, 1303 (2000).

[5] S.-K. Lee, J.-S. Kim, B. Kim, Y. Cha, W. K. Han, H. G. Min, Jikeun Seo, and S. C. Hong, Phys. Rev. B **65**, 014423 (2002); W. Wulfhekel, T. Gutjahr-Löser, F. Zavaliche, D. Sander, and J. Kirschner, *ibid.* **64**, 144422 (2001); H. L. Meyerheim, D. Sander, R. Popescu, J. Kirschner, P. Steadman, and S. Ferrer, *ibid.* **64**, 045414 (2001).

[6] M. Farle, W. Platow, A. N. Anisimov, P. Poulopoulos, and K. Baberschke, Phys. Rev. B **56**, 5100 (1997).

[7] P. Poulopoulos, P. J. Jensen, A. Ney, J. Lindner, and K. Baberschke, Phys. Rev. B **65**, 064431 (2002).

[8] R. K. Kawakami, Ernesto J. Escorcia-Aparicio, and Z. Q. Qiu, Phys. Rev. Lett. **77**, 2570 (1996); Hyuk J. Choi, Z. Q. Qiu, J. Pearson, J. S. Jiang, D. Li, and S. D. Bader, Phys. Rev. B **57**, R12713 (1998); R. K. Kawakami, M. O. Bowen, Hyuk J. Choi, Ernesto J. Escorcia-Aparicio, and Z. Q. Qiu, *ibid.* **58**, R5924 (1998).

[9] D. P. Pappas, K.-P. Kämper, B. P. Miller, H. Hopster, D. E. Fowler, A. C. Luntz, C. R. Brundle, and Z.-X. Shen, J. Appl. Phys. **69**, 5209 (1991); R. Allenspach and A. Bischof, Phys. Rev. Lett. **69**, 3385 (1992); R. Allenspach, J. Magn. Magn. Mater. **129**, 160 (1994).

[10] R. Pfandzelter and M. Potthoff, Phys. Rev. B **64**, 140405(R) (2001).

[11] E. Kisker, K. Schröder, W. Gudat, and M. Campagna, Phys. Rev. B **31**, 329 (1985); J. Kirschner, M. Globl, V. Dose, and H. Scheidt, Phys. Rev. Lett. **53**, 612 (1984); J. Kirschner, Phys. Rev. B **30**, 415 (1984).

[12] M. Pratzer and H. J. Elmers, Phys. Rev. B **69**, 134418 (2004).

[13] A. I. Lichtenstein, M. I. Katsnelson, and G. Kotliar, Phys. Rev. Lett. **87**, 067205 (2001).

[14] J. B. Staunton and B. L. Gyorffy, Phys. Rev. Lett. **69**, 371 (1992); S. S. A. Razee, J. B. Staunton, L. Szunyogh, and B. L. Györffy, Phys. Rev. B **66**, 094415 (2002); J. B. Staunton, S. Ostanin, S. S. A. Razee, B. L. Györffy, L. Szunyogh, B. Ginatempo, and Ezio Bruno, Phys. Rev. Lett. **93**, 257204 (2004).

[15] H. Hasegawa, J. Phys. F: Met. Phys. **16**, 347 (1986).

[16] H. Hasegawa, J. Phys. F: Met. Phys. **17**, 165 (1987).

[17] H. Hasegawa, Surf. Sci. **182**, 591 (1987).

[18] M. Pajda, J. Kudrnovský, I. Turek, V. Drchal, and P. Bruno, Phys. Rev. Lett. **85**, 5424 (2000); Phys. Rev. B **64**, 174402 (2001).

[19] F. López-Urías, G. M. Pastor, and K. H. Bennemann, J. Appl. Phys. **87**, 4909 (2000).

[20] T. Herrmann, M. Potthoff, and W. Nolting, Phys. Rev. B **58**, 831 (1998); J. H. Wu, H. Y. Chen, and W. Nolting, *ibid.* **65**, 014424 (2001).

[21] P. Bruno, Phys. Rev. Lett. **87**, 137203 (2001).

[22] M. Dantziger, B. Glinsmann, S. Scheffler, B. Zimmermann, and P. J. Jensen, Phys. Rev. B **66**, 094416 (2002).

[23] J. C. Neto, J. R. de Sousa, and J. A. Plascak, Phys. Rev. B **66**, 064417 (2002).

[24] H. Hasegawa, J. Phys.: Condens. Matter **1**, 9325 (1989).

[25] G. M. Pastor, J. Dorantes-Dávila, and K. H. Bennemann, Phys. Rev. B **40**, 7642 (1989).

[26] G. M. Pastor, J. Dorantes-Dávila, S. Pick, and H. Dreyssé, Phys. Rev. Lett. **75**, 326 (1995); J. Dorantes-Dávila and G. M. Pastor, *ibid.* **81**, 208 (1998); R. A. Guirado-López, J. Dorantes-Dávila, and G. M. Pastor, *ibid.* **90**, 226402 (2003).

[27] J. Hubbard, Phys. Rev. B **19**, 2626 (1979); **20**, 4584 (1979); H. Hasegawa, J. Phys. Soc. Jpn. **49**, 178 (1980); **49**, 963 (1980).

[28] J. A. Morkowski and P. Wosicki, J. Magn. Magn. Mater. **71**, 285 (1988).

[29] G. M. Pastor, J. Dorantes-Dávila, and K. H. Bennemann, Phys. Rev. B **70**, 064420 (2004).

[30] Olle Eriksson, A. M. Boring, R. C. Albers, G. W. Fernando, and B. R. Cooper, Phys. Rev. B **45**, 2868 (1992).

[31] A. Vega, J. Dorantes-Dávila, L. C. Balbás, and G. M. Pastor, Phys. Rev. B **47**, 4742 (1993).

[32] For the sake of clarity, a "hat" $(\hat{})$ is used to distinguish operators from numbers.

[33] J. C. Slater, *Quantum Theory of Atomic Structure, Vols. I and II* (McGraw-Hill, New York, 1960).

[34] J. B. Mann, Los Alamos Sci. Lab. Report LA-3690, 1967 (unpublished).

[35] B. Mühlschlegel, Z. Phys. **208**, 94 (1968).

[36] For simplicity, no prime is attached to $F(\vec{\xi},\vec{\eta})$ or $F(\vec{\xi})$ even though they derive from the effective single-particle Hamiltonian H'. The arguments of F should remove possible confusion with the thermodynamic function $F=-k_BT\ln Q$ associated to the many-body Hamiltonian H given by Eqs. (1)–(3).

[37] E. N. Economou, *Green's Functions in Quantum Physics*, *Springer Series in Solid State Sciences* (Springer, Heidelberg, 1983), Vol. 7.

[38] R. Haydock, in *Solid State Physics*, edited by H. Ehreinreich, F. Seitz, and D. Turnbull (Academic, New York, 1980), Vol. 35, p. 215. $\rho_{i\alpha\sigma}(E)=-1/\pi G_{i\alpha\sigma}$, where $G_{i\alpha\sigma}$ is the local Green's function.

[39] Y. Kakehashi and P. Fulde, Phys. Rev. B **32**, 1595 (1985).

[40] Y. Kakehashi and P. Fulde, Phys. Rev. B **69**, 045101 (2004).

[41] A. Enders, D. Peterka, D. Repetto, N. Lin, A. Dmitriev, and K. Kern, Phys. Rev. Lett. **90**, 217203 (2003).

[42] J. Dorantes-Dávila, H. Dreyssé, and G. M. Pastor, Phys. Rev. Lett. **91**, 197206 (2003).